PHYSICAL REVIEW B VOLUME 8, NUMBER 2 15 JULY 1973

Effects of Resonance Bonding on the Properties of Crystalline and Amorphous Semiconductors

G. Lucovsky and R. M. White
Xerox Palo Alto Research Center, Palo Alto, California 94304

(Received 30 November 1972)

The resonance aspect of chemical bonding is extended to solids with particular emphasis on its consequences for structural and vibrational properties. It is shown, for example, that the square of the infrared effective charge is proportional to the high-frequency dielectric constant in resonance-bonded systems. The IV-VI compounds and the group-VI elements are shown to exhibit the features of such resonance bonding. The dependence of resonance bonding on long-range order is discussed with respect to differences in the properties of the amorphous and crystalline phases of these materials.

I. INTRODUCTION

The physicist has traditionally sought a quantitative description of the optical and electronic properties of crystalline solids in terms of band theory. The recent work of Phillips[1-3] and his co-workers, principally Van Vechter,[4,5] has demonstrated the applicability of a chemical-bonding approach for a quantitative description of the properties of the tetrahedrally coordinated semiconductors. This work emphasized one aspect of the chemical bonding, the partial ionic character of the covalent bond between dissimilar elements which was characterized through an ionicity scale parameter f_i. This is a particular application of the more general concept of resonance[6] (sometimes called mesomerism[7]). The purpose of this paper is to extend the concept of resonance bonding to solids in general. We shall show that it provides a useful description for understanding certain properties of solids, particularly those related to structure. In Sec. II we consider in more detail the relation between the electronic and vibrational polarizabilities to be expected in a mesomerically bonded system. Then, in Sec. III we analyze the structure and infrared properties of the IV-VI compounds and group-VI elements and indicate how the concept of mesomeric bonding provides a natural explanation of certain properties such as very large infrared effective charges[8,9] and the linear relationship between the lattice and electronic polarizabilities.[9] Specific models for mesomeric bonding in these systems are discussed.

An important condition for the existence of resonance bonding in solids is the presence of long-range order. Therefore, we might expect materials which exhibit resonance bonding in the crystalline phase to have different properties in the amorphous phase. This is discussed in Sec. IV.

Resonance, as employed by the chemist, is an attempt to construct a many-body wave function as a linear combination of valence-bond configurations. Although such a basis is neither orthogonal nor complete, it provides a convenient qualitative description. Thus, if Φ_I and Φ_{II} are two such valence-bond configurations, the ground-state wave function ψ is approximated by

$$\psi = \frac{1}{(1+\alpha^2)^{1/2}} (\Phi_I + \alpha\Phi_{II}) \ , \qquad (1)$$

where the mixing coefficient α is determined by optionization of the binding energy. In extreme cases where α is either very small or very large, the most stable ground state is, respectively, I or II. In the more interesting cases where α is of order unity, the ground state of the system involves both structures, i.e., it is said to resonate between I and II. The binding energy of the resonant system is greater than either I or II; the difference in energy between the ground state and the more stable constituent structure is called the resonance energy.[6] Resonance is generally favorable only if each of the constituent structures has the same configuration of the nuclei and the same number of unpaired electrons.[10]

The most familiar bonding situation taken as an example of resonance is that of the benzene molecule, C_6H_6. The carbon-carbon distance in benzene is 1.39 Å which lies between that of the single- (1.54-Å) and double- (1.32-Å) bond lengths. Therefore, if one takes Φ_I and Φ_{II} to differ only in the location of the alternating double bonds, then one can choose α to account for the "abnormal" bond lengths. This points out one weakness in this approach; namely, by taking enough basis states, one can always introduce a sufficient number of adjustable parameters to explain a particular property. In practice however, the number of basis states can be restricted by energetic and symmetry conditions so that this weakness is at least in part overcome.

Aside from the structural implications of resonance, i.e., "abnormal" interatomic distances and bond angles, there are other manifestations of resonance present in both the chemical and physical properties. These include very large polarizabilities, both electronic and vibrational, as well as chemical properties that are different from those expected from any *one* of the constituent structures. A specific relationship between the electronic and vibrational polarizabilities is derived in Sec. II.

II. EFFECTIVE CHARGE IN RESONANTLY BONDED SYSTEMS

Structure in the infrared reflectivity is conveniently related to a Lorentzian oscillator model for the dielectric constant. The amplitude of this oscillator is characterized by an effective charge[8] e_T^*. In this section we shall investigate the effect of mesomeric bonding on the infrared effective charge. This macroscopic, or Born, charge e_T^* is defined by

$$e_T^* = \left(\frac{\partial P}{\partial u}\right)_E , \tag{2}$$

where P is the induced electric moment associated with the atomic displacement u. To calculate e_T^*, we shall consider a simple one-dimensional chain consisting of two different atoms per unit cell each of which contributes one electron to a resonating sp bond. This one-dimensional model does not restrict the generality of our result. The only essential requirement is that the optical vibration affect one of the valence-bond configurations differently than the other. The two basis states are shown in Fig. 1. Analytically these wave functions have the valence-bond form

$$\Phi_I = N \sum_R \sum_P (-1)^R R(-1)^P \times P\,\phi_{A1}(1)\,\alpha(1)\phi_{B1}(z)\beta(z)\cdots , \tag{3a}$$

$$\Phi_{II} = N \sum_R \sum_P (-1)^R R(-1)^P \times P\phi_{A'1}(1)\alpha(1)\phi_{B'1}(z)\beta(2)\cdots , \tag{3b}$$

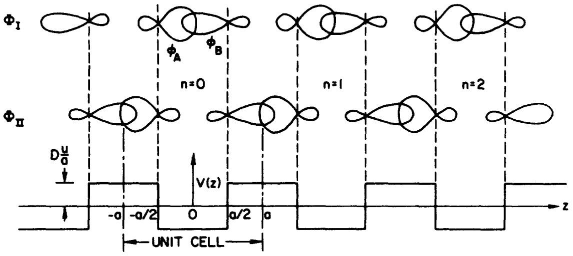

FIG. 1. One-dimensional model of a resonantly bonded system. The top two rows illustrate the two bonding configurations between which the system resonates. The bottom line shows the potential introduced by an optical phonon displacement with amplitude u. Here D is the deformation potential.

where N is a normalization factor, R interchanges spin functions, and P permutes the orbitals. Here $\Phi_{A,B}$ is a hybridized sp orbital. The primes refer to the oppositely directed orbitals shown in Fig. 1. As we indicated above, such a system is stabilized by adopting a resonant state of the form

$$\psi = \frac{1}{(1+\alpha^2)^{1/2}} (\Phi_I + \alpha\Phi_{II}) . \tag{4}$$

The coefficient α is determined by minimizing the total energy. If $\mathcal{H}$ is the Hamiltonian in the absence of any ionic displacement, this energy is $E(\alpha) = \langle\psi|\mathcal{H}|\psi\rangle$. In this case symmetry requires

$$\langle \Phi_I|\mathcal{H}|\Phi_I\rangle = \langle \Phi_{II}|\mathcal{H}|\Phi_{II}\rangle = \mathcal{H}_{11} \tag{5a}$$

and

$$\langle\Phi_I|\mathcal{H}|\Phi_{II}\rangle = \langle \Phi_{II}|\mathcal{H}|\Phi_I\rangle \equiv \mathcal{H}_{12} . \tag{5b}$$

Thus

$$E(\alpha) = \mathcal{H}_{11} + [2\alpha/(1+\alpha^2)]\mathcal{H}_{12} . \tag{6}$$

Minimizing with respect to α gives $\alpha_{\min} = -1$ ($\alpha_{\max} = +1$). Therefore $E_0 = \mathcal{H}_{11} - \mathcal{H}_{12}$ and we see $\mathcal{H}_{12}$ is the resonance energy we mentioned above.

Now consider the case of an ionic displacement characteristic of a long-wavelength optic phonon. At any given instant of time, the lattice will display a pair-wise "bunching" of the ions. As the ions move, the electrons will adapt to their instantaneous positions. This will lead to a redistribution of the electronic charge. In order to estimate this redistribution, we shall assume that the primary effect of the displacement is to produce a change in the potential seen by the electrons. This change will be proportional to the dilatation which, in this case, is u/a and the coefficient of proportionality is the deformation potential D. A square-well approximation of this strain-induced potential is illustrated in Fig. 1. Note that we are neglecting the actual displacement of the ions themselves. The total energy now becomes

$$E(\alpha) = \langle\psi|\mathcal{H} + D(u/a)|\psi\rangle = \mathcal{H}_{11} + \frac{2\alpha}{1+\alpha^2}\mathcal{H}_{12} + \frac{1-\alpha^2}{1+\alpha^2} D\frac{u}{a} . \tag{7}$$

Minimizing gives

$$\alpha = [1 + (Du/\mathcal{H}_{12}a)^2]^{1/2} - Du/\mathcal{H}_{12}a . \tag{8}$$

Let us now calculate the dipole moment associated with this redistribution of charge. If we wish to do this by taking the first moment of the charge density without having to worry about boundary effects, then we must choose the boundaries of our unit cell such that there is no polarization on them. In general, such a surface is difficult to ascertain.[11] However, in our one-dimensional case, symmetry considerations suggest that $z=\pm a$ are the appropriate boundaries. The charge density within this cell is

$$\rho(\vec{r}) = -\frac{|e|}{1+\alpha^2}\left(\Phi_I^* \Phi_I + \alpha^2 \Phi_{II}^* \Phi_{II}\right) + |e|\,\delta(\vec{r}+\tfrac{1}{2}a\hat{z}) + |e|\,\delta(\vec{r}-\tfrac{1}{2}a\hat{z}) \,. \tag{9}$$

Noting the axial symmetry, the dipole moment becomes

$$P = [(1-\alpha^2)/(1+\alpha^2)](P_A - P_B) \;, \tag{10}$$

where $P_{A,B}$ is the dipole moment associated with the sp orbital. This shows explicitly that the moment is zero for a homopolar material. Using the result (8) for α and the definition (2), we obtain

$$e_T^* = (D/\mathcal{H}_{12})(P_A - P_B)/a \;. \tag{11}$$

This result contains a number of interesting features. First of all, it involves the resonance energy $\mathcal{H}_{12}$. From a molecular orbital approach based on the directed orbitals $\phi_{A,B}$ plus the Mulliken approximation relating off-diagonal matrix elements of the form $\langle\phi_A|\mathcal{H}|\phi_B\rangle$ to diagonal matrix elements and overlap integrals one can show that the resonance energy is proportional to the average energy gap E_g. Therefore, since the optical frequency dielectric constant of a semiconductor has the form $\epsilon_\infty = 1 + (\hbar\omega_p/E_g)^2$ this predicts that $(e_T^*)^2 \sim (\epsilon_\infty - 1)$: ω_p is the plasma frequency for the valence electrons. Since the dielectric constant varies over a wider range than the other parameters in Eq. (11), we expect this relationship to provide a strong indication of the existence of resonance bonding in an isoelectronic series. One of the attractive features of this result is that it involves parameters that have physical relevance and can be determined experimentally. One could derive an effective charge from, say, a shell model but the result would involve a set of parameters which are model dependent.

Another feature of this result is that the order of magnitude of this effective charge can vary from a very small value to as large as several times e. This may be seen by taking the case in which orbital A is a $6s6p$ hybrid while orbital B is a $3s3p$ hybrid. For this case

$$P_A - P_B \simeq \left(1 - \frac{\bar{r}(n=3,\, l=1)}{\bar{r}(n=6,\, l=1)}\right)\frac{1}{2}\,ea = \frac{3}{8}\,ea \;. \tag{12}$$

For deformation potentials of the order of 10 eV with gaps of the order of 1 V or less, we find $e_T^*/e \sim 4$.

III. APPLICATION TO CRYSTALLINE SOLIDS

A. IV-VI Compounds

The IV-VI compounds occur in three structures at STP; the rocksalt (NaCl) structure, and rhombohedral and orthorhombic distortions of that structure. We shall here emphasize the properties of the NaCl structure crystals SnTe, PbS, PbSe, and PbTe. (GeTe occurs in the rhombohedral structure; GeS, GeSe, SnS, and SnSe occur in the orthorhombic structure.)

If we consider the nonmetallic NaCl crystals, then SnTe and the Pb chalcogenides have very different properties when compared to other materials that crystallize in the same structure. For example, the alkali halides and and alkaline-earth materials are wide band-gap (> 3 eV) insulators, whereas SnTe and the Pb salts are narrow band-gap (> 0.5 eV) semiconductors; the alkali halides are very soluble in water, to the extent that they are hydroscopic whereas the IV-VI compounds are totally insoluble in water.

The interatomic distances in the alkali halides and alkaline-earth crystals can be understood in terms of an ionic model in which ionic radii are assigned to the constituent atoms and in which the equilibrium spacing is determined primarily by Coulomb forces.[6] In Table I we compare the interatomic distances in the Pb chalcogenides with those calculated from the ionic radii.[12] The agreement is generally poor, in particular when compared to a similar analysis of the interatomic distances in the alkali halide crystals. In Table II we also include interatomic distances calculated from metallic radii.[13] In all cases, the crystalline interatomic distance is intermediate between the two calculated distances, the one based on ionic radii and the one based on metallic radii. We have not attempted comparisons based on covalent radii due to the fact that the IV-VI compounds do not have a sufficient number of valence electrons available for covalent bonding at octahedral sites. If we make an assumption at this point, that the bonding in PbS is intermediate between ionic and metallic, then the wave function has the form of Eq. (1) where Φ_I represents the ionic state and Φ_{II} represents the metallic state. The parameter α could

TABLE I. Comparison of the crystalline Pb-chalcogenide-atom interatomic distance with distances calculated from ionic radii and metallic radii. f_i' is an ionicity defined by Eq. (13); f_i'' is an ionicity defined in Ref. 14.

	M-X distance (Å)				
Material	Crystal	Ionic radii	Metallic radii	f_i'	f_i''
PbS	2.97	3.04	2.54	0.86	0.77
PbSe	3.06	3.18	2.67	0.76	0.72
PbTe	3.22	3.41	2.87	0.65	0.63

TABLE II. Comparison of nearest- and next-nearest-neighbor distances in the stable (STP) forms of S, Se, Te, and two of the metastable forms of Se. Also included in the table are comparisons of d_1 with twice the normal covalent radius, and d_2 with twice the van der Waals radius.

Material	Nearest-neighbor distance, d_1 (Å)	Next-nearest-neighbor distance, d_2 (Å)	d_2/d_1	$d_1/2r_c$ r_c= covalent radius	$d_2/2r_V$ r_V= van der Waals radius
Orthorhombic S	2.06	3.50	1.70	0.99	0.95
Trigonal Se	2.37	3.44	1.45	1.01	0.86
Trigonal Te	2.84	3.50	1.23	1.04	0.80
α-monoclinic Se	2.34	3.80	1.62	1.00	0.95
Amorphous Se	2.34	3.75	1.60	1.00	0.94

then be used to define an ionicity. Or, equivalently, one can define an ionicity, f'_i, based on the interatomic spacing in the crystal d_{AB}, and idealized spacings calculated from ionic d^I_{AB}, and metallic d^M_{AB}, radii, i.e.,

$$f'_i = \frac{d_{AB} - d^M_{AB}}{d^I_{AB} - d^M_{AB}} . \tag{13}$$

These ionicity parameters are included in Table I where they are compared with ionicities calculated by Stiles and Brodsky.[14] Stiles and Brodsky developed an ionicity scale f''_i for the ten-electron (per atom pair) diatomic crystals that is an analog of the Phillips-Van Vechten[3,4] scale. The two ionicity scales, (f'_i, f''_i) rank the materials in the same order, i.e., the ionicity decreasing in going from PbS to PbSe to PbTe, and are in relatively good quantitative agreement. For SnTe, it is impossible to make comparisons of this sort, since the ionic radius for Sn^{2+} is calculated from the interatomic spacing in SnTe.

It is well known that both the electronic $(\epsilon_\infty - 1)$ and lattice (e_T^{*2}) polarizabilities of the IV-VI compounds are unusually large[8,15]; here ϵ_∞ is the real part of the optical frequency dielectric constant and e_T^* is the macroscopic infrared effective charge which characterizes the strength of the reststrahlen and is in turn proportional to the contribution of the lattice modes to the static dielectric constant. Lucovsky, Martin, and Burstein[9] noted that in the IV-VI NaCl crystals, that $e_T^* \sim \epsilon_\infty$; in Fig. 2 we replot their results and find that the points can be fit by an equation

$$(e_T^*)^2 = a(\epsilon_\infty - 1) , \tag{14}$$

where $a \sim 1$. This agrees with the result derived in Sec II.

We have thus far shown that the NaCl IV-VI compounds display all of the "anomolous" properties of a resonance system; i.e., their properties are not consistent with a simple ionic picture (very small band gap and insolubility in water), their interatomic spacings are intermediate to those calculated from pure bond-type models, and their electronic and lattice polarizabilities are unusually large and satisfy Eq. (14). Before invoking a particular model for the resonance bonding that is suggested for these materials,[7] we illustrate a similar situation that prevails in the group-VI elements.

B. Group-VI Elements

Table II contains the nearest (d_1) and next-nearest (d_2) neighbor distances for the stable (STP) phases of the group-VI elements S, Se, and Te. The bonding in these materials, in particular, orthorhombic S and trigonal Se, is frequently described by a molecular-crystal model, wherein the nearest-neighbor bonding is covalent and the next-nearest-neighbor bonding is by van der Waals-type forces. In Table II we compare d_1 with twice the neutral atom covalent radius[6] $(2r_c)$ and d_2 with twice

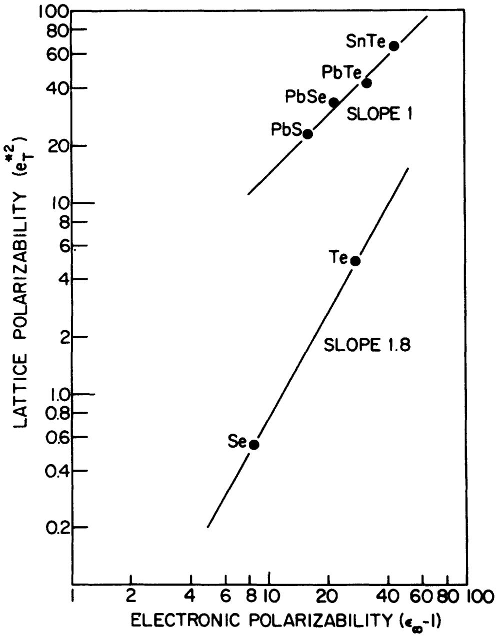

FIG. 2. Plots of the lattice polarizability (e_T^{*2}) vs the electronic polarizability $(\epsilon_\infty - 1)$ for the IV-VI NaCl crystals and for trigonal Se and trigonal Te.

the van der Waals radius[6] ($2r_V$). Note here that as we go from S to Se to Te,[16] $d_1/2r_c$ increases, whereas $d_2/2r_V$ decreases, suggesting that the nearest-neighbor bonding becomes weaker and less covalent, and that the next-nearest-neighbor bonding becomes stronger. This systematic relationship between crystal interatomic spacings and calculated idealized interatomic spacings is again suggestive of resonance bonding. In Table II we have also included similar comparisons for two metastable forms of Se, α-monoclinic Se and amorphous Se. In both cases, the molecular-crystal-type description of the bonding is better than in the stable form of Se, trigonal Se.

Figure 2 also contains values of $(e_T^{*2})_{av}$ and $(\epsilon_\infty - 1)_{av}$ for trigonal Se and Te. If a power-law relationship between $(e_T^{*2})_{av}$ and $(\epsilon_\infty - 1)_{av}$ of form (14) is assumed, the proportionality factor a is about an order of magnitude smaller than in the IV-VI compounds. Preliminary measurements on orthorhombic S indicate a small value of e_T^* consistent with the trends we have identified in Se and Te.

C. Resonance-Bonding Model

Much of the description of resonance bonding in these materials follows directly from the discussions given in Ref. 7. As we pointed out in Sec. III A on the IV-VI compounds, the crystalline interatomic distances suggest that bonding in the IV-VI compounds is intermediate between ionic and metallic bonding. A similar conclusion concerning a metallic contribution to the bonding in the IV-VI compounds was reached by Lucovsky, Martin, and Burstein[9] from an analysis of the lattice dynamical parameters, the elastic constants, and optic-mode frequencies. In a resonance picture there are two important structures to consider. One of these is an ionic structure, Pb^{2+} and S^{2-}; the second is a metallic structure. In the ionic structure, Pb gives its p electrons to S, so that

$$\begin{aligned} &\mathrm{Pb}\,(6s^2\,6p^2) \longrightarrow \mathrm{Pb}^{2+}(6s^2)\ , \\ &\mathrm{S}\,(3s^2\,3p)^4 \longrightarrow \mathrm{S}^{2-}\,(3s^2\,3p^6)\ . \end{aligned} \tag{15}$$

For this case, the S^{2-} ion achieves the closed-shell electron configuration of the rare gas argon, whereas the Pb^{2+} ion has a non-rare-gas electron configuration. In the metallic picture, a resonance or mesomeric bonding scheme is achieved through incomplete occupancy of the six pair bonds between each atom and its neighbors. In this picture,

$$\begin{aligned} &\mathrm{Pb}\,(6s^2\,6p^2) \longrightarrow \mathrm{Pb}^-\,(6s^2\,6p^3)\ , \\ &\mathrm{S}\,(3s^2\,3p^4) \longrightarrow \mathrm{S}^+\,(3s^2 3p^3)\ , \end{aligned} \tag{16}$$

where the p electrons from bonds between the S and Pb atoms for only three of the six neighbors located in orthogonal directions. Since there is an ambiguity as to which neighbor is chosen in these pair bonds, i.e., in the $\langle 100 \rangle$ direction whether it is in the + or − sense, one must invoke a resonance configuration which is achieved only in the presence of long-range order. If we use a line (—) to indicate pair bonds, involving, in this case, overlapping p orbitals from neighboring Pb and S atoms, then we have a description of the following sort:

$$\mathrm{Pb{-}S\ Pb{-}S\ Pb{-}S} \rightleftarrows \mathrm{Pb\ S{-}Pb\ S{-}Pb\ S}\ . \tag{17}$$

Since 12 electrons are necessary for pair bonding at octahedral sites, the six-electron (or half-satisfied bonding) description leads to a metallic structure. As Krebs[7] has pointed out this type of resonance is not possible in SrS where the Sr atom electron configuration is $5s^2$. The resonance description implicit in Eq. (17) requires p orbitals on both of the atoms; for Sr the use of these orbitals is unfavorable since they are well removed in energy from the other valence states of the system. In contrast, for the IV-VI crystals, the occupancy of p orbitals in both the neutral Pb and S atoms favors a resonance picture.

As was pointed out earlier, the usual bonding picture for the group-VI elements is one in which the nearest neighbors in either the ring or chains are covalently bonded, and in which the rings or chains are held together in a crystalline array by van der Waal-type forces. It is well known that this description holds better for orthorhombic S than for trigonal Se or Te. In the molecular-crystal model, each of the chalcogenide atoms makes two covalent bonds to its near neighbors and contributes its remaining four electrons to lone-pair orbitals. The two bonding orbitals and one of the lone pairs have (approximately) sp^2 symmetry, and the second lone pair p symmetry, so that in this picture, for example,

$$\mathrm{Se}(4s^2\,4p^4) \longrightarrow \mathrm{Se}(sp^2)^4 p^2\ . \tag{18}$$

In the resonance picture of the bonding in trigonal Se and trigonal Te, the second configuration is a metallic structure in which an additional pair bond is formed between next-nearest neighbors in adjacent chains. These additional pair bonds have the helical symmetry of the chain structure, and, as in the IV-VI compounds, require long-range order. In this resonance description, the creation of Se ions (Se^+, Se^-) is required. Paralleling the resonance description in CO_2,[6] on a time average all atoms are neutral so that the ionicity is dynamic. The existence of dynamic ionicity in the resonance picture for trigonal Se and trigonal Te does, however, help one to understand the dynamic origin of the large effective charges in these elemental

TABLE III. Comparison of bond lengths in crystalline and amorphous GeSe and GeTe.

Material	Bond length amorphous phase (Å)	Bond length crystalline phase (Å)	Bond length from covalent radii (Å)
GeSe	2.35[a]	2.71(2), 2.70(1)[c] 2.95(2), 2.96(1)	2.37
GeTe	2.6[b]	2.92(3)[c] 3.02(3)	2.58

[a] Reference 20.

[b] Reference 19.

[c] R. W. G. Wyckoff, *Crystal Structures*, 2nd ed. (Interscience, New York, 1963), Vol. 1.

crystals.[17,18]

In each of the examples given above, resonance effects occur in situations where there are an insufficient number of electrons to satisfy the orbitals required for covalent bonding, i.e., it occurs in unsaturated structures and is therefore almost a direct antithesis of the more familiar bonding situations in molecules. In the molecular cases where resonance occurs, there are usually too many electrons present to satisfy pair bonding so that the resonance occurs in the π rather than in the σ orbitals.[6] In the case of PbS, there are only ten electrons per atom pair, whereas 12 are required for saturated covalent bonding. In the case of Se and Te, the local site symmetry is that of a distorted octahedron, so that 12 electrons per atom pair are also required for saturation. There are indeed 12 electrons available; however, their symmetries are not matched to the orbitals required for octahedral coordination (d^2sp^3). The fact that Po occurs in the simple cubic structure and is a metal rather than a semiconductor, supports this argument concerning the necessity of d orbitals for covalent bonding at octahedral sites.

IV. APPLICATION TO AMORPHOUS SEMICONDUCTORS

In Sec. III we demonstrated the applicability of a resonance-bonding model for an interpretation of some of the properties of the IV-VI compounds and group-VI elemental crystals. In each of the examples, the interatomic spacings could not be accounted for in a simple way, i.e., they were intermediate, in the case of the IV-VI compounds, between values that would be expected from either purely ionic or purely metallic bonding. In Table II we have included values of d_1 and d_2 for two *metastable* forms of Se, α-monoclinic Se and amorphous Se. In each of these materials, d_1 is smaller than d_1 in trigonal Se, and d_2 is larger so that the ratios $d_1/2r_c$ and $d_2/2r_V$ are closer to unity. In effect, these metastable forms of Se are more molecular than trigonal Se. In our resonance picture their metastability can be attributed to the absence of resonance effects; i.e., the additional binding energy in trigonal Se results from the interchain resonance. Since this resonance requires long-range order, and a favorable geometric arrangement of polymeric extended chains or molecular units, it is indeed more pronounced in the trigonal form. The resonance-bonding picture is also consistent with other differences between trigonal Se, and α-monoclinic and amorphous Se. For example, the optical frequency dielectric constant in amorphous Se is 6 and is smaller than that of trigonal Se (7.7 for $\vec{E} \perp c$ axis and 12.8 for $\vec{E} \parallel c$ axis). The contributions of the lattice modes to the static dielectric constant in trigonal Se are also substantially higher (~factor of 100) than in amorphous or α-monoclinic Se.

In the IV-VI compounds similar differences occur between the amorphous and crystalline counterparts. In this case, the bonding in the distorted NaCl-structured materials, e.g., GeS, GeSe, and GeTe, is a resonance stabilized covalent-metallic system[7,15] which leads to approximately three near and three next-nearest neighbors. In the amorphous phases of these materials, radial distribution studies indicate interatomic spacings that are substantially less than in the crystals.[19,20] In Table III we compare the bond lengths d_1 for crystalline and amorphous GeSe and GeTe. For the amorphous phases d_1 is approximately equal to the sum of the covalent radii of Ge and the appropriate chalcogenide atom. For the crystalline materials, the two values of d_1 for each material are intermediate between the appropriate sum of ionic and metallic radii. The lattice frequencies of the Ge chalcogenides also reflect the large differences in the chemical bonding between the crystalline and amorphous phases. We have studied the far-infrared reflectivity of a polycrystalline sample of GeSe and have found a single very strong reststrahlen band. The resonance (or TO phonon) frequency is 160 cm^{-1} and the contribution of this mode to the dielectric constant is comparable to that of the TO-phonon mode in PbS. Table IV contains the characteristic Ge-S, Ge-Se, and Ge-Te vibrational mode frequencies for the amorphous phases of these materials as obtained by Hilton *et al.*[21] They have also studied alloys of Ge and the chalcogenide atoms with other glass-forming elements, e.g., As and

Si, and have confirmed that these frequencies are indeed characteristic of the bond-stretching modes.

For amorphous GeSe, Hilton *et al.* report a resonance frequency of 234 cm^{-1}; this is substantially different from our value of 160 cm^{-1} for crystalline GeSe. We have also studied a polycrystalline sample of GeS_2; this crystal has the SiO_2 structure in which each Ge atom is fourfold coordinated and each S atom is twofold coordinated. By comparing our spectra for GeS_2 with those for SiO_2, we have identified the characteristic Ge-S stretch frequency to be approximately 335 cm^{-1}. This is very close to the frequency of Ge-S bonds in the amorphous material as studied by Hilton *et al.* and leads us to conclude that the bonding in the amorphous Ge chalcogenides is described by the four-two coordination that would be expected if the Ge and chalcogenide atoms were bonded according to the rules of classical valence chemistry. This argument for local valence bond satisfaction can be further substantiated by comparing the vibrational frequencies of the amorphous Ge chalcogenides with the stretch mode frequencies of the gaseous Ge tetrahalides. This comparison is included in Table IV. Also included in that table are similar comparisons for amorphous As_2S_3 and As_2Se_3 and their respective molecular analogs, $AsCl_3$ and $AsBr_3$. The comparisons in Table IV are based on a molecular model[22,23] for the vibrational frequencies of amorphous chalcogenides. For the As chalcogenides, the molecular unit is an AsX_3 pyramidal molecule (X = chalcogenide atom); for the Ge chalcogenides, the unit is a tetrahedral GeX_4 molecule. The comparison of the stretch mode frequencies yields a ratio of approximately 0.82 for the As compounds and 0.74 for the Ge compounds. The important aspect of the comparison is that the frequency ratio is essentially the same for the three pairs of Ge compounds, and for the two pairs of As compounds. The ratio is less than one due to electronegativity differences between the adjacent chalcogen and halogen atoms, i.e., S and Cl, Se, and Br, and Te and I. For the group IV-VI materials, the interatomic distances and characteristic vibrational frequencies are both consistent with a substantial change in the local order in going between the crystalline and amorphous phases.

TABLE IV. Comparison of the stretch-mode vibrational frequencies of amorphous GeS, GeSe, GeTe, As_2S_3, and As_2Se_3 with those of their respective molecular analogs.

Amorphous material	Vibrational frequency ν_A(cm^{-1})	Molecular analog	Vibrational frequency ν_G(cm^{-1})	ν_A/ν_G
GeS	349[a]	$GeCl_4$	453[c]	0.77
GeSe	234[a]	$GeBr_4$	328[c]	0.71
GeTe	196[a]	GeI_4	264[c]	0.74
As_2S_3	309[b]	$AsCl_3$	370[c]	0.84
As_2Se_3	218[b]	$AsBr_3$	275[c]	0.79

[a] Reference 21.

[b] References 22 and 23.

[c] G. Herzberg, *Molecular Spectra and Molecular Structure* (Van Nostrand, New York, 1945), Vol. II.

In summary, for the amorphous and crystalline elemental chalcogenides, Se and Te, the major difference in chemical bonding is a change in second-neighbor effects. In our description the change is brought about by a loss of long-range order, and hence the inability to achieve a resonance in the interchain bonding. For the IV-VI compounds in general, and for the Ge chalcogenides in particular, the change in bonding between the amorphous and crystalline phase has a more striking effect on both the coordination number and the nearest-neighbor bond length. For Se and Te, there is no change in coordination number and only a very small change, for Se, in the bond length.

V. CONCLUSIONS

We have used a bonding model to account for certain "anomolous" or special properties of two classes of crystalline solids, the IV-VI compound and group-VI elemental semiconductors. In each of these cases a resonance picture was invoked wherein there were two possible electronic configurations. The resonance in each case requires long-range order and in this way accounts for some of the large differences in properties between the amorphous and crystalline forms of these materials.

It is important to place the bonding picture into proper prospective with respect to a band description. In a band calculation, one starts with some basis such as plane waves, atomic orbitals, etc, and determines the energy as a function of wave vector. From the resulting eigenfunctions one can determine the charge density as a function of position within a unit cell. The bonding approach represents a zeroth-order approximation to this spatial distribution. If these two descriptions are to be consistent, then the symmetries of the orbitals of which the chemical bond is constructed must also appear in the valence-band Bloch functions. Thus, for example, if we have octahedral bonds of the form d^2sp^3 a band calculation might show d-like character at certain symmetry points, p like and s like at others. These zeroth-order hybrid orbitals could also serve as a basis for a quantitative band calculation. An example of this approach is to be found in Chen's recent calculation for selenium.[24] Of course, if the calculation is carried far enough the result should be independent of the original basis. Thus a bond description is particularly useful for semiconductors and metallic like materials where the concept of spatially directed bonds is well defined. In a real metal involving nearly free electrons, such a description would not be appropriate.

A final point concerns the use of ionicity scales for the description of the chemical bonding in solids. The Phillips-Van Vechten[3,4] scale f_i and the Stiles-Brodsky[14] scale f_i'' base their definitions of ionicity on the antisymmetric components of the atomic pseudopotentials. They imply pure covalent bonding at one end of the scale, $f_i, f_i'' = 0$, and pure ionic bonding at the other, $f_i, f_i'' = 1$. In our description of mesomeric bonding in the NaCl-structured IV-VI crystals, we used a model [see Eq. (13)] wherein $f_i' = 1$ implied ionic bonding but $f_i' = 0$ implied metallic bonding. The point to emphasize here is that there are three types of contributions to the chemical bonding in solids: ionic, covalent, and metallic, and that all three of these should be considered in the development of "ionicity scales." There are instances wherein a two-dimensional field may be adequate, e.g., the bonding in the group-VI elements can be discussed in terms of covalent and metallic bonding where f_i, the covalency, is approximately one for orthorhombic S and zero for Po. However, there are other systems, e.g., the distorted (with respect to NaCl) IV-VI compounds (GeS, GeSe, GeTe, SnS, and SnSe), wherein all three contributions should be considered.

---

[1] J. C. Phillips, Phys. Rev. Lett. 19, 415 (1967).

[2] J. C. Phillips, Phys. Rev. Lett. 20, 550 (1968).

[3] J. C. Phillips, Phys. Rev. 168, 905 (1968).

[4] J. C. Phillips and J. A. Van Vechten, Phys. Rev. Lett. 22, 705 (1969).

[5] J. A. Van Vechten, Phys. Rev. 182, 891 (1969).

[6] L. Pauling, *The Nature of the Chemical Bond*, 3rd ed. (Cornell U.P., Ithaca, N. Y., 1960).

[7] H. Krebs, *Fundamentals of Inorganic Crystal Chemistry* (McGraw-Hill, London, 1968).

[8] E. Burstein, A. Pinczuk, and R. F. Wallis, in *Proceedings of the Conference of the Physics of Semimetals and Narrow Gap Semiconductors*, edited by D. L. Carter and R. T. Bate (Pergamon, New York, 1971), p. 251.

[9] C. Lucovsky, R. M. Martin, and E. Burstein, Phys. Rev. B 4, 1367 (1971).

[10] This latter consideration holds in molecules, but is not necessarily strictly obeyed in solids.

[11] R. M. Martin (private communication).

[12] L. V. Azaroff and J. J. Brophy, *Electronic Processes in Materials* (McGraw-Hill, New York, 1963).

[13] L. Pauling, *The Chemical Bond* (Oxford U.P., London, 1967).

[14] P. J. Stiles and M. H. Brodsky, Solid State Commun. 11, 1063 (1972).

[15] G. Lucovsky, R. M. Martin, and E. Burstein, in Proceedings of the Conference on the Physics of IV-VI Compounds and Alloys, Philadelphia, Pa., 1972 (unpublished).

[16] G. Lucovsky, Phys. Status Solidi B 49, 633 (1972).

[17] G. Lucovsky, R. C. Keezer, and E. Burstein, Solid State Commun. 5, 439 (1967).

[18] I. Chen and R. Zallen, Phys. Rev. 173, 833 (1968).

[19] F. Betts, A. Bienenstock, and S. R. Ovshinsky, J. Non-Cryst. Solids 4, 554 (1970).

[20] D. E. Sayers, F. W. Lytle, and E. A. Stern, J. Non-Cryst. Solids 8-10, 401 (1972).

[21] A. R. Hilton, C. E. Jones, R. D. Dobratt, H. M. Klein, A. M. Bryant, and T. D. George, Phys. Chem. Glasses 7, 116 (1966).

[22] G. Lucovsky and R. M. Martin, J. Non-Cryst. Solids 8-10, 185 (1972).

[23] G. Lucovsky, Phys. Rev. B 6, 1480 (1972).

[24] I. Chen, Phys. Rev. B 7, 3672 (1973).

PHYSICAL REVIEW B VOLUME 8, NUMBER 2 15 JULY 1973

Threshold Characteristics of Interband Electronic Raman Scattering

S. Srivastava and K. Arya

Tata Institute of Fundamental Research, Bombay-5, India

(Received 26 September 1972)

Interband electronic Raman scattering for excitations from the light-hole band to the heavy-hole band in p-type InSb and from the valence band to the conduction band in n-type gray tin has been studied. The effect of the residual Coulomb interaction between the Bloch electrons has been incorporated by treating it within the framework of the random-phase approximation, and by including the vertex correction due to the final-state electron-hole interaction. Both the effects of the Coulomb interaction are found to play significant roles in enhancing the scattering cross section near the thresholds.

I. INTRODUCTION

In recent years the intraband electronic Raman scattering, in which electrons are excited by light within the same band, has been studied extensively by various authors.[1,2] The effect of the residual Coulomb interaction is usually included in such studies within the framework of the random-phase approximation (RPA).[2] It leads to the well-known screening of single-particle excitations due to charge-density fluctuations in degenerate semiconductors. In such a case, for momentum trans-